[17] J. M. White, D. K. Winslow, and H. J. Shaw, "Time reversal and correlation at 1.35 GHz using nonlinear interaction in a bulk acoustic-wave device," *Proc. IEEE* (Lett.), vol. 60, pp. 1102–1103, Sept. 1972.
[18] M. Yamanishi and T. Kawamura, "Acoustic-surface wave convolver using nonlinear electron interactions in coupled semiconductor-piezoelectric systems," in *Proc. 1972 IEEE Ultrasonics Symp.*, pp. 288–291, Oct. 1972.
[19] J. L. Bleustein, "A new surface wave in piezoelectric materials," *Appl. Phys. Lett.*, vol. 13, pp. 412–413, Dec. 15, 1968.
[20] Yu. V. Gulayev, "Electroacoustic surface waves in solids," *JETP Lett.*, vol. 9, no. 37, Jan. 5, 1969.
[21] A. R. Hutson and D. L. White, "Elastic wave propagation in piezoelectric semiconductors," *J. Appl. Phys.*, vol. 33, pp. 40–47, Jan. 1962.
[22] D. K. Winslow, H. J. Shaw, and J. M. White, "Acoustic parametric interactions," Stanford Univ., Stanford, Calif., Semiannu. Rep. F30602-71-C-0125, Microwave Lab. Rep. 2108, Oct. 1972.
[23] C. E. Cook and M. Bernfeld, *Radar Signals—An Introduction to Theory and Application.* New York: Academic Press, 1967, p. 197.

Signal Processing by Electron-Beam Interaction with Piezoelectric Surface Waves

ALAIN G. BERT, BERNARD EPSZTEIN, AND GÉRARD KANTOROWICZ

Abstract—**A new type of device is described in which an acoustoelectric surface wave interacts with low energy free charges created on the surface of a piezoelectric material. The experimental results obtained show that one of the most promising applications is an analog RF storage device for which several minutes of storage time have been achieved at 30 MHz on quartz with an internal insertion loss of 63 dB. If the width of the current pulse is large enough, direct attenuation of the surface wave may be measured due to the energy absorbed by the motion of secondary electrons. Experimental and theoretical results are presented. The limitations and the applications of the device to signal processing are discussed.**

I. Introduction

BULK and surface acoustic waves are both used in signal processing, but surface waves are generally more versatile because of their accessibility. This feature is particularly important on piezoelectric substrates: the wave can be coupled to the external medium through the electric field associated with it. We discuss here some interactions between the electric field and free charges moving in vacuum near the surface. The free charges may be created either by a cathode (or photocathode) or by secondary emission. In any case their mean energy must be small, i.e., of the order of magnitude of the potential associated with the acoustic wave, in order to allow the electric field of the wave to modify the trajectories of the primary or secondary electrons and/or to change the amount of created charges. Three kinds of devices can be derived from this principle.

1) By processing the resulting current modulation, one may use the device as an electronic acoustic wave transducer.

2) When the resulting modulation of the charge density is made to create an electrostatic image of the acoustic wave on an insulating surface, which may be the surface of the piezoelectric substrate itself, the device will be able to store the acoustic signal and achieve associated functions, such as time inversion.

Manuscript received October 4, 1972; revised November 3, 1972. This work was supported in part by the Direction des Recherches et Moyens d'Essais, Paris, France, under Contract 71/194.
The authors are with the Laboratoire de Recherches Hyperfréquences, Groupement Tubes Electroniques, Thomson-CSF, Orsay, France.

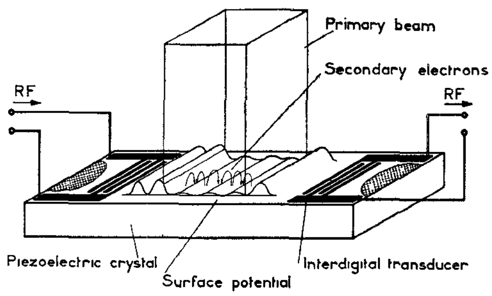

Fig. 1. Schematic diagram of acoustic signal storage device.

3) Cumulative interaction between the electric potential of a surface wave and adjacent free electrons can produce either an attenuation or an amplification on an acoustic wave.

Examples of the first type of devices have been given by a number of authors. The detection of a piezoelectric field by modulation of secondary electrons emitted by an electron beam of a few hundred volts impinging on a piezoelectric plate immersed in an acoustic field, is used in the Sokolov ultrasonic camera [1] for visualization of an acoustic field.

Electron-beam sensing of a surface elastic wave has been considered in order to provide an electronically variable delay line [2], but the results published up to now have not yet proved whether this approach could be successful.

The present paper is primarily concerned with the two other types of devices for which first experimental results have been given in a recent paper [3]. A schematic diagram of the operation is given in Fig. 1. An electron beam accelerated at a few hundred volts is made to impinge upon the entire surface of a piezoelectric crystal. Its current density may be varied from zero to tens of milliamperes per square centimeter. Input and output interdigital transducers are deposited on the surface. The beam current is pulse modulated. A metallic shield prevents electrons from hitting the fingers of the transducers. After an RF signal has been fed through the input transducer, the surface is flooded by the electron beam during a few nanoseconds. After a delay which may be as long as 1 min, the electron beam hits the surface once again during the same time. A replica of the original signal is then obtained from the output transducer and a time inversion of the same signal is obtained from the input transducer. The main process involved in this device is the effect of the electric field associated with the acoustic surface wave on the redistribution of the secondary electrons. The existence of this effect has been first observed in an experiment which will be described in Section II where direct absorption of an acoustic wave results from its cumulative interaction with an electron beam. Some theoretical results for the writing–reading processes of the storage device will then be given and compared with experimental measurements. Limits and signal processing capabilities of the device will also be discussed.

The arrangement shown in Fig. 1 is by no means the only possible configuration. For instance, instead of a short current pulse a sheet electron beam may be shifted across the crystal.

Also, the acoustical wave may be guided and/or excited by other types of transducers. Trains of current pulses may be used instead of only one. As a result, the signal processing capabilities of this device are numerous. Among them, the acoustical static memory and the complete time inversion of a signal are the most novel applications.

II. Preliminary Experiment

The effect of the electric field of a surface acoustic wave on the secondary electrons may be shown by the following experiment. The apparatus is essentially the same as described for Fig. 1, but the width of the current pulse can take on values greater than the transit time of the wave between transducers.

The experiment was performed on quartz and on lithium niobate. Fig. 2 shows the result obtained at 14 MHz on quartz. The area flooded by the electron beam was 3 cm long, corresponding to a transit time for the Rayleigh wave of about 10 μs. The total delay between transducers was 13 μs. The shape of the output signal may be explained as follows. If secondary electrons are accelerated by the electric field of the wave, they must extract energy from the acoustic wave. Therefore, a decrease in the amplitude of the output signal must be observed when the beam is on. Let A and B refer to the edges of the illuminated area, A located toward the input transducer, B toward the output transducer. t_B is the time of arrival at plane B, and t_1 is the time at which the current pulse starts. As may be seen in Fig. 2, the part of the wave which arrives at plane B at $t_B \leq t_1$ has not suffered any absorption; the part of the wave which arrives at plane B at any time t_B such that $t_2 \leq t_B \leq t_3$ has been attenuated by the interaction with secondary electrons during its entire transit from A to B. Each part of the wave which arrives at B between t_1 and t_2 was located between A and B when the current pulse started. Let C be this location: absorption has appeared only between C and B. The same argument holds for $t_3 \leq t_B \leq t_4$ showing that this portion must be symmetrical to the portion $t_1 \leq t_B \leq t_2$. Fig. 3 shows results obtained at 14 MHz on lithium niobate for two values of the current density, the dimensions of the illuminated area being the same as before. Two remarks must be made concerning these results. First, it appears here that the amplitude of the wave decreases exponentially with time. Secondly, the attenuation may reach almost 100 percent for a sufficiently high current density. The exponential decrease is not particular to lithium niobate: it may be explained if one

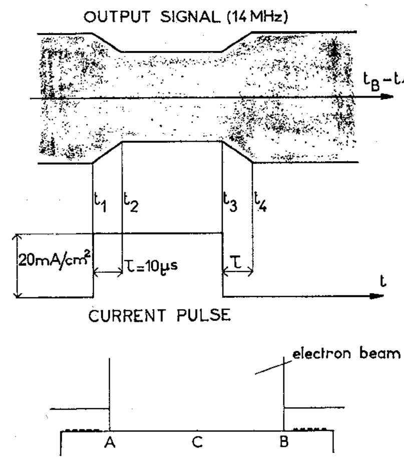

Fig. 2. Direct attenuation of 14-MHz surface acoustic wave on quartz due to interaction of associated electric field with free electrons. Output signal position is shown relative to current pulse. Illuminated area is 3 cm long.

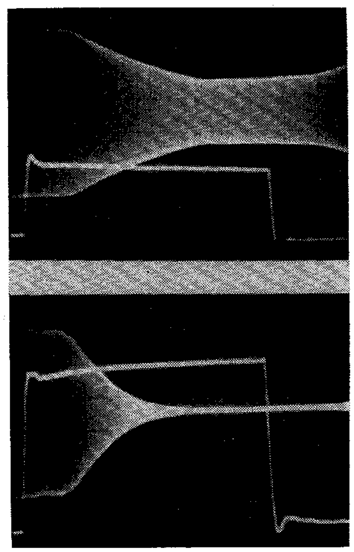

Fig. 3. Observed absorption of 14-MHz surface acoustic wave on lithium niobate for two values of the current density. Time scale 2 μs/div. Input power was 1 W. Current densities are, respectively, 40 and 90 mA/cm².

assumes that the power absorbed by the electrons between x and $x+dx$ is proportional to the power crossing the yz plane, the x axis being parallel to the acoustic propagation

$$\frac{dP(x)}{dx} = -\alpha P(x)$$

where α is a function of the primary current density J_p. Only a small part of the exponential decrease can be observed with quartz. The total insertion loss was measured as a function of beam current. Results are reported in Fig. 4. These results show that the maximum attenuation suffered by the acoustic wave is a function of k^2, the surface electromechanical coupling coefficient.

There is therefore an experimental evidence of the influence of the acoustic wave on the electron redistribution process. In another experiment, we have taken advantage of this effect to obtain a storage device.

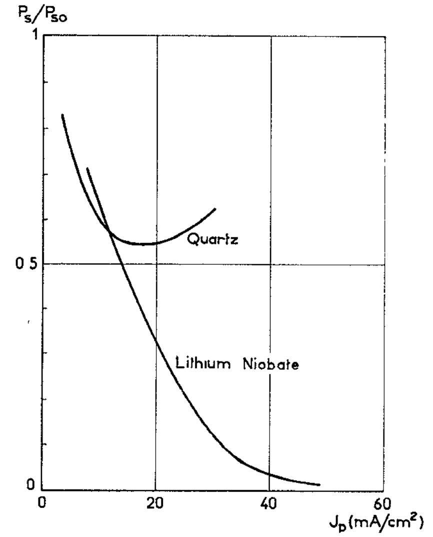

Fig. 4. Maximum absorption of 14-MHz surface acoustic wave on quartz and lithium niobate as a function of current density. Illuminated area is 3 cm long.

III. Writing and Reading Processes in a Storage Device

Let us suppose that the primary electron beam strikes the surface during a time short with respect to the RF period (Fig. 1). Secondary electrons are generated, the energy of which is of the order of a few electronvolts. Therefore, their trajectories depend on the electric potential distribution of the wave, which is also of the order of a few volts at the surface, for 100-mW/cm acoustic power. The secondary electrons that turn back toward the piezoelectric crystal will no longer be uniformly distributed. Clearly they are attracted by the regions which are at a positive potential. While the wave moves on, the charge pattern remains frozen. The maximum recorded signal corresponds to the situation at the point where the electrical potential is completely canceled at the surface by the charges which are deposited. The electrostatic potential amplitude is then equal to the amplitude of the potential associated to the wave.

A charge image is then obtained which can be stored during a long time depending on surface conductivity or unwanted parasitic charge deposits. A similar situation is found in storage tubes where a signal may be restituted hours after being written.

By means of the reverse piezoelectric effect, the electric field created by the charges induces mechanical stresses in the substrate. Suppose a second current pulse is triggered. For the duration (assumed short) of the pulse, the situation is the same as during the first current pulse except that the electric potential is created by the stored charges and not by an acoustic wave. Therefore the electric potential on the surface is suddenly reduced or canceled. The stresses are also reduced or canceled in a very short time, giving rise to two waves propagating in opposite directions. Reading is thus achieved.

Let us look into writing and reading processes in more detail. Suppose that, while an acoustic wave is on the surface, the electron beam starts to hit the crystal at time $t=0$. The total electric potential distribution on the surface V is the sum of the electric potential due to the surface acoustic wave (amplitude V_s) and the potential created by the charges deposited on the surface (amplitude V_q). V may be written $V=V_i+V_a\cos(\beta x-\omega t)$. Actually, we shall first analyze the system during a time that is short with respect to the period so that

$$V \simeq V_i + V_a \cos \beta x.$$

The calculation of the redistribution of the secondaries on the surface is rather involved. A first approach would be to compute the trajectories of a certain number of secondaries, starting from several positions x_1 on the surface, with various energies and angles. An element of current between two adjacent trajectories remains constant, so that only the landing positions x_2 are needed to obtain the redistributed current density. The precision of the computation is determined by the distance between adjacent landing positions which must be much less than one acoustical wavelength. Unfortunately, it turns out that most secondaries travel a long distance before falling back on the surface. Therefore, a large number of trajectories are needed.

We shall follow an alternate approach which may be obtained from a simplified model. If we note that 1) the electric field is symmetrical with respect to the planes $x=n\lambda_s$ where λ_s is the acoustical wavelength and that 2) if V_a is changed to $-V_a$, the sign of all the sinusoidal terms in the redistributed current is changed, it turns out that the total current collected by the surface may be written in the following form:

$$J = J_{s0}\left[a_0 - 1 + \frac{1}{\delta} + a_1 \frac{V_a}{V_0}\cos\beta x + \text{terms in}\left(\frac{V_a}{V_0}\right)^m \text{and } \cos n\beta x\right] \quad (1)$$

where $m>2$ and $n>1$ with

$$J_{s0} = \delta(1-R)J_p. \quad (2)$$

Here δ and R are the coefficients of secondary emission and backscattering, V_0 is the most probable energy of the secondary electrons, J_p is the primary beam current density, and the coefficients a_0 and a_1 are functions of V_i and J_p, a_0 being the redistribution coefficient when $V_a=0$.

The following analysis will be limited to the small signal case [terms in $(V_a/V_0)^m$ will be neglected]. The terms in $\cos n\beta x$ will also be neglected since they correspond to harmonics which will not be in the passband of the output transducer.

Let C be the capacitance per unit area of the surface with respect to the surrounding electrodes and Γ the surface capacitance per unit area. Γ is defined in Appendix II where it is shown to be equal to $\beta\epsilon_0(1+\epsilon')$, ϵ' being the effective relative permittivity of the substrate. The time variation of the surface potentials is given by the following expression:

$$J\,dt = C dV_i + \Gamma dV_a \cos\beta x$$

or

$$C\frac{dV_i}{dt} = J_{s0}\left[a_0 - 1 + \frac{1}{\delta}\right] \quad (3)$$

$$\Gamma\frac{dV_a}{dt} = a_1 J_{s0}\frac{V_a}{V_0}\cdot \quad (4)$$

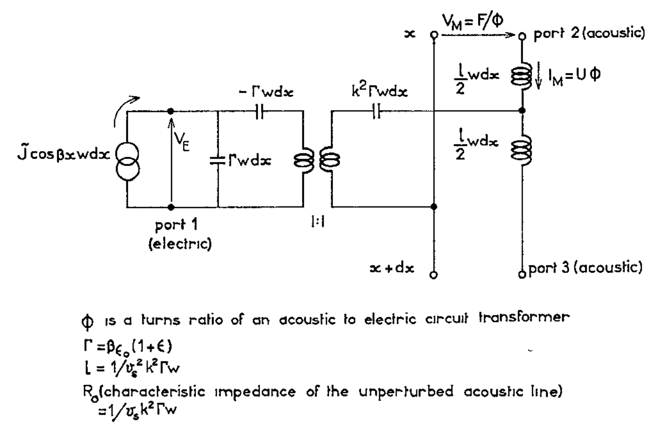

Fig. 5. Equivalent circuit of electron-beam–surface-wave interaction.

Note that V_a is negative since the charges tend to decrease V_a. The first equation has been solved by Wendt [5] with the assumption of a Maxwellian distribution.

For example, suppose that $\delta = 2.5$, $V_0 = 3$ V, $C = 1$ pF/cm², $R = 0.2$, $J_p = 10$ mA/cm². If at $t = t_1$, V_i is equal to $\pm 2V_0$, it turns out that the equilibrium value will be attained in about 1 ns. This time is generally short compared to the time that V_a takes to reach its equilibrium value. We could otherwise suppose that the surface has been flooded by a pulse of electrons before the acoustic wave propagates. The coefficient a_1 can therefore be considered as a constant so that

$$V_a = V_s \exp\left(-\frac{\tau}{\tau_1}\right) \tag{5}$$

where

$$\tau_1 = \frac{-\Gamma V_0}{a_1 J_{s0}}. \tag{6}$$

This means that the potential $V_q \cos \beta x$, created by the redistributed charges, tends to cancel the potential of the surface wave $V_s \cos \beta x$ with an exponential decrease in time. If τ is the width of the current pulse, at the end of the pulse V_a will be equal[1] to $V_s \exp(-\tau/\tau_1)$ which means that charges have been deposited on the surface, giving rise to a potential distribution

$$(V_a - V_s) \cos \beta x = -V_s(1 - \exp(-\tau/\tau_1)) \cos \beta x. \tag{7}$$

This expression gives the amplitude of the recorded signal.

The reading process may be described with the help of an equivalent circuit (Fig. 5) derived from the well-known Mason model. Across port 1, the voltage $V_E = V_{E0}$ is given by (7). A current pulse is triggered. During a short time τ, the voltage V_E decreases to a value which will be:

$$\begin{aligned} V_E &= V_{E0} \exp(-\tau/\tau_2) \\ &= -V_s(1 - \exp(-\tau/\tau_1)) \exp(-\tau/\tau_2) \cos \beta x \end{aligned}$$

where τ_2 is the same as τ_1 except for the value of J_p which may be different for reading. One may therefore consider that a step function has been applied to port 1, the amplitude of which is:

$$\Delta V_E = V_{E0}(1 - \exp(-\tau/\tau_2)).$$

V_{E0} is the potential due to the charges deposited during the writing process. ΔV_E is the potential due to the charges deposited during the reading process. Therefore, $V_E = V_{E0} - \Delta V_E U(t)$, where U is the step function. Solving the equations of the circuit, one finds the value of the output power after reading P_s' versus V_s^2 which in turn can be related to the power P_s of the recorded wave [6]. The intrinsic loss η of the writing–reading process is then obtained:

$$\eta = \frac{P_s'}{P_s} = \frac{k^4}{4}(1 - \exp(-\tau/\tau_1))^2(1 - \exp(-\tau/\tau_2))^2. \tag{8}$$

If τ is not negligible compared to the period, an additional multiplicative term $F(\tau)$ must be introduced

$$F(\tau) = \left(\frac{\sin \omega\tau/2}{\omega\tau/2}\right)^4.$$

It is interesting to note that the maximum value of P_s'/P_s is $k^4/4$, depending only on the value of the surface electromechanical coupling coefficient. Materials having a high value of k^2 seem therefore advantageous. However, let us consider an example. Suppose that the current density is adjusted to a value for which $\tau_1 = \tau$ with quartz. If a lithium niobate substrate is used instead of quartz with the same current density and pulse length as before, τ_1 which is proportional to $(1+\epsilon')$ is about 20 times greater [see (6)], whereas k^2 also is 20 times greater. Therefore,

$$\frac{\eta_{\text{niobate}}}{\eta_{\text{quartz}}} \simeq 1.6 \times 10^{-2}.$$

If we desire $\eta_{\text{niobate}} > \eta_{\text{quartz}}$, the current density must be more than three times greater for niobate than for quartz. Therefore, the advantage of the large value of k^2 is paid by the need of a much higher beam current due to the fact that generally the maximum value of k^2/ϵ remains almost constant for most materials. In all the preceding discussion, it has been assumed that the time spent by the secondaries to become redistributed over the surface is small compared to the period. An electron moving at a velocity of 3 eV covers a distance of 33 wavelengths during one tenth of a period. The approximation is correct if a grid is placed close to the surface at a distance h less than 10–20 wavelengths. If no grid is placed close to the surface, the space charge potential minimum has an equivalent effect, but the distance h of the virtual grid is then a function of the primary current density. In this case, if J_p is too small, a_1 will be much smaller than the value obtained by the previous analysis because most electrons will take a time close to the period to become redistributed over the surface.

A similar analysis can be derived for the absorption process as described in Section II. One writes that the total surface potential

$$V_a(t) \exp(j\omega t)$$

is the result of the addition of the electric potential of the surface wave and of the potential created by the sum of all the charges deposited from the beginning of the current pulse.

[1] This analysis is valid only if τ_1 and the width τ of the current pulse are short with respect to the period. If τ is not negligible compared to the period, a_1 must be multiplied by $\sin(\omega\tau/2)/\omega\tau/2$.

The redistributed current is then derived from (1). The power extracted per unit of x is proportional to the product of the redistributed current by the surface potential. The time variation of the amplitude of the delayed CW wave is found to be given by (Appendix I)

$$P_s(t) = P_{s0} \exp\left(-\frac{k^2\omega t}{\omega\tau_1 + (1/\omega\tau_1)}\right).$$

This expression gives the decrease of power with time at the plane where the wave leaves the illuminated area $t=0$ corresponding to the starting time of the current pulse. Here t is the time spent by the wave under the influence of the electron beam. This exponential decrease may be observed on the experimental results of Figs. 2 and 3. P_s reaches a minimum value $P_s(T_d)$ when the width of the current pulse τ is larger than the time delay T_d corresponding to the illuminated area. As J_p is varied, $P_s(T_d)$ passes through a minimum value for a value of J_p given by $\omega\tau_1=1$.

IV. Experimental Results of Acoustic Signal Storage

Experiments have been performed on quartz at 30 MHz. Quartz has some advantages over other possible materials: it offers good resistance to thermal changes and is a good insulator. Furthermore, its dielectric constant is low, so that a signal may be recorded and read with relatively small values of beam current density. The electron beam is grid-modulated, the grid being designed for short pulse modulation. Reading and writing are achieved with current pulses of equal width, with independently variable amplitudes. The acoustic structure does not differ very much from usual surface delay lines: the aluminum-deposited interdigital transducers are 10 acoustic wavelengths long. Care must be taken to prevent electrons from impinging on the fingers of the transducers or on the RF connections. Otherwise, two parasitic RF pulses appear at the output on each side of the restituted RF signal. One of these parasitic pulses is due to the impulse excitation of the output transducer caused by the reading current. The other is due to the same effect on the input transducer, which appears delayed and smaller at the output.

An insertion loss of 60 dB defined as the power ratio of the signal read after storage to the signal delayed between the two transducers is calculated using a k^2 of 2×10^{-3}. Measurements give 62–64 dB with a current pulse width of 10 ns ($\omega\tau=0.6\pi$), which is close to the calculated value.

The storage time may be increased by applying the cathode voltage during only a few tens of microseconds while writing and reading. This has been found necessary because grid emission was important: its temperature was high due to the use of an impregnated cathode. Fig. 6 shows observed variations in the shape of the signal after 3, 5, 7, and 9 min of storage. Aside from the influence of residual interpulse current, the surface resistivity is of major importance. The decay time τ_M of the recorded signal due to the surface conductivity is given by

$$\tau_M = \frac{\epsilon_0(1+\epsilon)}{\beta}\rho_s$$

where ρ_s is the surface resistivity.

The signal obtained from the input transducer that is the time-inverted image of the original signal is shown in Fig. 7.

(a)
(b)
(c)
(d)

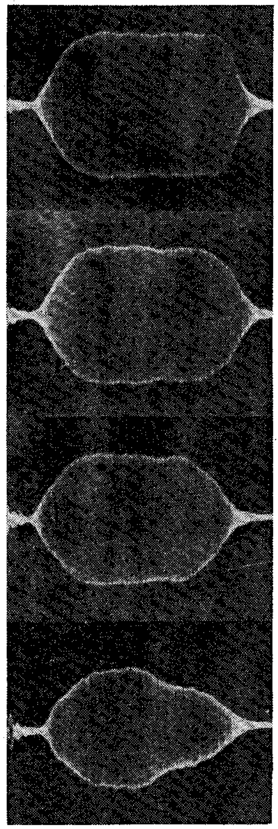

Fig. 6. 30-MHz stored signal restituted after (a) 3 min. (b) 5 min. (c) 7 min. (d) 9 min of storage. Time scale 1 μs/div.

(a)
(b)
(c)

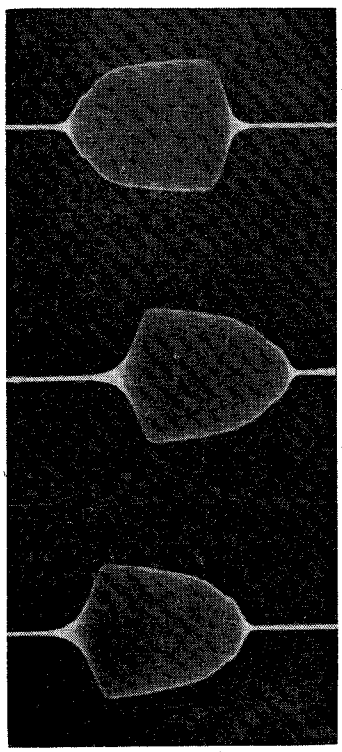

Fig. 7. Output signals at 30 MHz. Scale is 1 μs/div. (a) Delayed signal without recording. (b) Signal obtained from output transducer after storage time of 160 ms. (c) Time-inverted signal obtained from input transducer after same storage time as in (b).

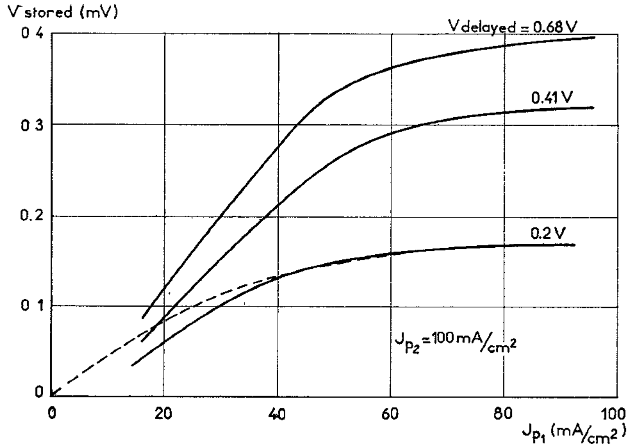

Fig. 8. Measured amplitude of stored signal versus writing current density at 30 MHz, for different values of input power. Reading current density is 100 mA/cm². Theoretical result for small signal approximation is given by dotted curve.

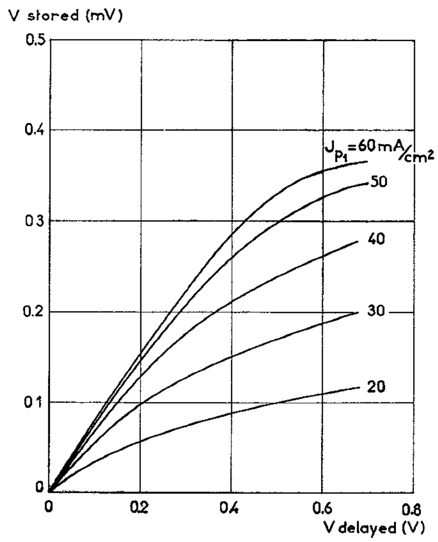

Fig. 9. Amplitude of resituted signal after storage versus amplitude of delayed signal.

The curves of Fig. 8 give the measured amplitude of the output signal as a function of the writing current density for a given reading current and for different values of the input signal. The amplitude of the output signal when the device is used as a simple delay line is 0.2, 0.41, and 0.68 V. The reading current density is 100 mA/cm². The storage time is 18 ms. A theoretical curve is shown for the delayed signal of 0.2 V with the condition $a_1(1-R)\delta/V_0=1$. The experimental results seem to lead to the conclusion that a_1 is not constant with J_p and turns out to be lower for small values of the current density. One reason for this has already been mentioned: if the retarding field due to the space charge is not large enough, most secondaries take a time of the order of the RF period to redistribute over the surface. However, this mechanism alone cannot explain such a variation.

In Fig. 9 the amplitude of the restituted signal after storage is plotted versus the amplitude of the delayed signal for different values of the writing current density. It appears that if the current is large enough, the device is linear up to $V_{\text{delayed}}=0.5$ V, which corresponds to an input power of 300 mW or to an amplitude of the electric potential associated with the acoustic wave of about 1.2 V. For lower values of the current density, it appears that the limit of linearity decreases. This nonlinearity is due to the storage process, the quartz being linear throughout the signal level range. The preceding theory assumes small signal conditions, and for large values of input power, the higher order terms in V_a/V_0 are no longer negligible.

It has been verified that the phase of the original RF signal was also restituted without distortion. Comparison of photographs of both signals has shown the same carrier frequency. The dynamical range of the restituted signal is better than 40 dB.

V. Limits of the Storage Capability

In the experiment described in the preceding section, on quartz, a signal of 10-μs duration has been stored at 30 MHz with an intrinsic loss of about 60 dB. These figures can be improved.

The maximum realizable crystal size usually precludes the storage of a signal longer than about 30 μs without complicating the device. The following two ways offer a possibility of improvement in this matter: sequential recording and waveguiding to lengthen the acoustic path.

Fig. 10 is an example of the first solution. The crystal surface is divided with separated parallel acoustic channels. The electron-beam area covers only one path at a time and can be swept across the total surface, writing sequentially the signal in successive channels. Reading is achieved in exactly the same manner. Metallic strips are deposited between successive acoustical paths that may be biased in order to prevent secondary electrons from erasing the signal stored in adjacent paths.

Another solution consists of lengthening the acoustical path by guiding the wave, as shown schematically in Fig. 11. Here, the beam impinges upon the entire surface. Two difficulties are inherent to this solution. First, bulk wave generation makes the attenuation greater. Second, the electromechanical coupling coefficient is not constant along the waveguide. Therefore, the restituted signal will be distorted in amplitude. However, this variation may be compensated by adequately modulating the current density across the surface.

A storage time of about 1 h or more seems feasible. It depends on 1) the resistivity of the piezoelectric substrate, 2) the surface cleanliness during operation, 3) the amount of parasitic charges deposited between the writing and the reading current pulses. The minimum delay between writing and reading is limited by parasitic echoes of the input signal. Surface and bulk wave echoes may be observed. The former are minimized as usual by suitably matching the transducers and depositing absorbing pads at the ends of the crystal, bearing in mind that all materials employed must be compatible with the presence of a cathode. The latter are due to reflexions at the bottom and at the ends of the crystals of bulk waves generated by the input transducer. 50–100 μs are realizable figures for the minimum delay before reading, with reasonable signal-to-noise ratio.

The current density necessary to store and restitute a signal with the same potential amplitude on the same substrate is proportional to the square of the frequency. This F^2 law can be obtained from the expression giving the insertion loss which

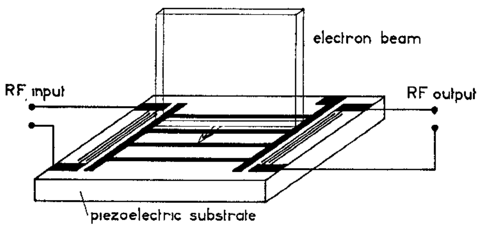

Fig. 10. Storage of long signals by sequential recording.

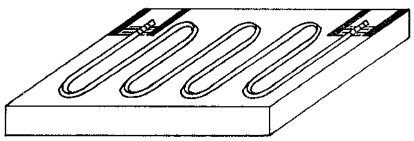

Fig. 11. Storage of long signals by waveguiding.

is a function of $\omega\tau$ or $\omega\tau_1$. Indeed, the amount of charge q necessary to store a certain amplitude of the wave is proportional to the electric field which in turn is proportional to the frequency. Now, the duration τ of the current pulse is inversely proportional to the frequency. Therefore, the current $I=q/\tau$ must vary as F^2. The current density has been shown to be of the order of tens of milliamps per square centimeter on quartz at 30 MHz. A device working at 100 MHz needs therefore hundreds of milliamps per square centimeter with pulsewidths of the order of 2–3 ns. This fact sets up a practical limit for the operating frequency.

However, this limit may be overcome if, instead of unique pulses, one uses trains of N pulses at a repetitive rate equal to the central operating frequency of the transducers. The current density can then be divided by N. This advantage is obtained at the expense of relative bandwidth which otherwise would only be limited by the transducers.

Another approach to decrease the needed current density is to deposit on the surface a thin film of material having a high secondary emission coefficient.

As already mentioned, piezoelectric materials with high values of the electromechanical coupling coefficient also have high values of the dielectric constant. Consequently, the current density must be much higher to take advantage of the large k^2 coefficient to decrease the intrinsic losses of the writing–reading process. The difficulty turns out to be the same as for an increase in frequency, and pulse trains may be used to overcome it.

Still another method could use the enhancement of the charge stored signal by differential secondary emission obtained with a slow primary electron beam between writing and reading [7]. When the electron-beam energy is near the first value for which $\delta=1$, the positive slope of the secondary emission curve causes the electron current leaving a region where the potential is greater to be higher than the current leaving a region where the potential is lower. The potential difference is therefore increased, thus effecting a gain in the stored charge.[2] An increase by a factor of 10–20 of the amplitude of the recorded signal seems feasible. This *in situ* amplification makes it also possible to have successive readings without significant decrease in amplitude, the stored signal, attenuated by a partial reading, being amplified previous to the next reading. Great improvements in the storage time capability can also be achieved in the same way. The amplitude of the signal is restored with a periodicity corresponding to a certain amount of the self-erasing time.

[2] Note that the same process could be used to amplify directly an acoustic wave, provided the secondaries are prevented from redistributing on the surface, for instance, by placing a grid very close to it or by immersing the device in a magnetic field.

VI. Other Signal Processing Capabilities

The interaction between an electron beam and surface acoustic waves may have many applications in signal processing. The capability of the device to store an RF signal can be used as an acoustical static memory from a few tens of microseconds up to minutes. One may notice that the delay does not depend on temperature. Among its many potential applications this device allows to make the convolution between two signals separated by a long and unknown time lag. The first signal is recorded, and its reading is triggered by the second signal. Both the delayed first signal and the second signal are fed into the convolver.

As another example, time compression may be obtained for fast processing of low rate data pulses. Here the electron beam has just the dimension corresponding to the length of each pulse. The first pulse is recorded close to the output transducer. The beam is shifted by one step toward the input transducer. The second signal is then recorded, and so on. The reading is achieved on all the surface at once.

Addition or substraction of signals separated by a long time lag can be obtained with the arrangement shown in Fig. 10. The first signal is stored in the first acoustic channel. The beam is shifted on the second channel where the second signal is then stored. Both channels are read simultaneously so as to add (or subtract according to the phase that has been chosen) through the output transducer.

Another important application is the time inversion obtained from the input transducer. Here the whole signal is time inverted, not only its amplitude. Such a device could be useful if applied to the processing of linear FM pulses.

Spectrum analysis of a single signal can also be achieved. Suppose that by some means the frequency spectrum of the signal can be spatially distributed along the surface of a piezoelectric crystal.[3] A first current pulse impinges upon all the surface, recording the total signal. The frequency spectrum of the signal can be obtained by successive reading with a sheet beam shifted along the surface.

Besides signal storage and time inversion, the direct absorption of an acoustic wave described in Section II may be used for attenuation, modulation, or switching of acoustic signals.

Also, the modulation of the secondary electron current by the electric potential of the surface wave can be used as an electronic transducer [2]. The efficacy of such a device depends essentially on the size of the electron beam. If the beamwidth is of the order of a quarter of an acoustic wavelength, the RF signal may appear in the secondary electron collector current. An arrangement based on this idea is shown in Fig. 12. Secondary electrons are collected by a grid placed close and

[3] Such a situation is obtained in the RAC device [8].

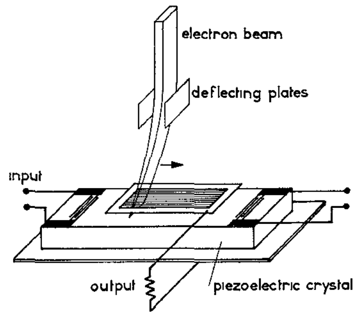

Fig. 12. Electronically variable delay line.

parallel to the surface. A very thin sheet electron beam impinges upon the surface, perpendicular to the direction of acoustical propagation, and can be deflected along this direction. The main feature of such an arrangement is that it constitutes a delay line continuously variable from almost zero to tens of microseconds.

VII. Conclusions

The interaction between an electron beam and acoustic surface waves on piezoelectric substrates has been discussed. Theoretical analysis and experimental results have shown that the acoustoelectric field modulated redistribution of low energy secondary electrons allows a new approach to signal processing, adding by these means to the already available methods of utilization of surface acoustic waves. Signal storage and time inversion obtained in this way seem to have no equivalent in currently available signal processing techniques. Examples illustrating the possibilities of this kind of interaction show a promising new field of interest for acoustic components.

Appendix I

Direct Absorption of an Acoustic Wave When the Width of the Current Pulse is Large

The surface potential varies as $V_a(t) \exp(j\omega t)$. V_a is the result of the addition of the electric potential of the surface wave V_s and the potential created by the sum of all the charges deposited from the beginning of the current pulse

$$V_a \exp(j(\omega t - \beta x)) = V_s \exp(j(\omega t - \beta x)) + \frac{1}{\Gamma}\int_0^t a_1 J_{s0} \frac{V_a}{V_0} \exp(j(\omega t - \beta x))\, dt$$

which gives

$$V_a = \left[\frac{\exp - \left(j\omega + \frac{1}{\tau_1}\right)t}{1 + j\omega\tau_1} + \frac{1}{1 + \frac{1}{j\omega\tau_1}}\right] V_s.$$

If t is large compared to the period,

$$V_a \simeq \frac{V_s}{1 + \frac{1}{j\omega\tau_1}}.$$

The amplitude of the alternating part of the redistributed current density is therefore

$$\tilde{J} = J_{s0} a_1 \frac{V_s/V_0}{1 + \frac{1}{j\omega\tau_1}} = -\frac{\Gamma V_s}{\tau_1} \frac{1}{1 + \frac{1}{j\omega\tau_1}}.$$

The power absorbed between x and $x+dx$ is

$$dP_s = \tfrac{1}{2} R_e(V_a \tilde{J}^* w\, dx)$$

where w is the width of the acoustic beam or

$$dP_s = -\frac{1}{2}\frac{\Gamma V_s^2}{\tau_1} \frac{1}{1 + \left(\frac{1}{\omega\tau_1}\right)^2} w\, dx. \tag{9}$$

V_s^2 is related to the power of the acoustic wave by the following relation [6]:

$$P_s = \frac{\omega\epsilon_0(1 + \epsilon')}{2k^2} w V_s^2 = \frac{\omega\Gamma}{2\beta k^2} w V_s^2.$$

Integrating (9) gives the variation of the wave power along its direction of propagation,

$$P_s = P_{s0} \exp\left[-\frac{k^2\beta x}{\omega\tau_1 + \frac{1}{\omega\tau_1}}\right].$$

$x = 0$ corresponds to the entrance plane of the wave into the illuminated area. The preceding relation then gives the law of decrease of the acoustic power with distance along the surface. This relation may also be expressed as a function of time

$$P_s = P_{s0} \exp\left[-\frac{k^2\omega t}{\omega\tau_1 + \frac{1}{\omega\tau_1}}\right].$$

The energy ΔU_s absorbed per unit area is $\Delta U_s = (1/\omega)(dP_s/w\, dx)$ which may be written, according to (9),

$$\Delta U_s = -\frac{U_E}{\omega\tau_1 + \frac{1}{\omega\tau_1}}$$

where $U_E = \frac{1}{2}\Gamma V_s^2$ is the electric energy density associated with the unperturbed acoustic wave.

Therefore, the maximum energy density that can be extracted from the wave is $U_E/2$. When $J_p = 0$, $\Delta U_s = 0$ since there is no redistributed current; when J_p tends to infinity, ΔU_s still tends to zero since now V_a tends to zero.

Appendix II

Surface Capacitance

In order to compute the unit surface capacitance, let us suppose that we have deposited at the surface $z = 0$ the following charge density distribution:

$$q = q_0 \exp(j\beta x)$$

with an infinite extent in the xy plane, and let us compute the voltage distribution created by the surface charges by assuming that we have a semi-infinite crystal in the negative z direction and empty space for z positive.

Above the crystal, the potential distribution is given by

$$\phi' = V_a \exp(j\beta x - \beta z).$$

If it is assumed that the crystal is weakly piezoelectric as in the case of quartz, the potential inside the crystal is given by

$$\phi = V_a \exp(j\beta x + \beta z).$$

The condition to be fulfilled at the surface by the normal components of the electric induction in empty space D_2' and in the crystal D_2 is

$$D_2' - D_2 = q.$$

Always neglecting the piezoelectric effect, on a Y-cut quartz with the X direction oriented along the x axis, this may be written

$$\epsilon_0 \beta V_a + \epsilon_{zz} \beta V_a = q_0.$$

This expression allows the definition of the unit surface capacitance as

$$\Gamma = \frac{q_0}{V_a} = \epsilon_0 \beta [1 + \epsilon_{zz}/\epsilon_0].$$

In a more general case, with different crystal cuts, or with a crystal having a much higher piezoelectric coupling than quartz, this formula holds by using ϵ_{zz}/ϵ_0 instead of a more involved expression ϵ' taking into account other components of the dielectric tensor or some of the piezoelectric constant [4]

$$\epsilon' = \frac{1}{\epsilon_0} \sqrt{\epsilon_{zz}\epsilon_{xx} - \epsilon_{zx}^2} + \text{piezoelectric terms.}$$

ACKNOWLEDGMENT

The authors wish to thank Prof. P. Guenard for stimulating discussions during the course of this study, and P. Vial, B. Gerber, R. Valat, and J. Oisel for their technical assistance.

REFERENCES

[1] S. Ya. Sokolov, "The ultrasonic microscope," *Nature* (USSR), vol. 9, pp. 45–48, Sept. 1949.
[2] M. Epstein, S. G. Joshi, R. J. Serafin, and A .P. van den Heuvel: "Electron beam sensing of surface elastic waves," *Proc. IEEE* (Lett.), vol. 58, pp. 253–254, Feb. 1970.
[3] A. G. Bert, B. Epsztein, and G. Kantorowicz, "Charge storage of acoustic RF signals," *Appl. Phys. Lett.*, vol. 21, July 15, 1972.
[4] H. Engan, H. Hanebrekke, K. A. Ingebrigtsen, and E. Jergan, "Numerical calculations on surface waves in piezoelectrics," *Appl. Phys. Lett.*, vol. 15, Oct. 15, 1969.
[5] G. Wendt, "Charge et décharge d'un isolant par émission secondaire dans les tubes à mémoire," *Ann. Radioelec.*, vol. 13, pp. 316–325, Oct. 1958.
[6] K. M. Lakin, "Perturbation theory for electromagnetic coupling to elastic surface waves on piezoelectric substrates," *J. Appl. Phys.*, vol. 42, pp. 899–906, Mar. 1, 1971.
[7] A. S. Jensen, M. P Siedband, and I. Limansky, "*In situ* amplification of a signal stored upon a dielectric surface," *IEEE Trans. Electron Devices*, vol. ED-16, pp. 30–35, Jan. 1969.
[8] R. C. Williamson and H. I. Smith, "Large time bandwidth product surface wave pulse compressor employing reflective gratings," *Electron. Lett.*, Aug. 10, 1972.

Application of Acoustic Surface-Wave Technology to Spread Spectrum Communications

DeLAMAR T. BELL, JR., JERRY D. HOLMES, AND RICHARD V. RIDINGS

Invited Paper

Abstract—**Spread spectrum transmission is being proposed for an increasing number of digital communication, navigation, and radar systems. One of the reasons is the simplicity and availability of surface-wave devices (SWD) for performing the necessary signal generation and processing. The properties of spread spectrum signals, the operation of SWD's, and their advantages and limitations when used in communication systems are discussed. Spread spectrum terminology and basic concepts are defined in terms common to both systems engineers and device designers.**

I. INTRODUCTION

SPREAD spectrum transmission is a form of signal processing which trades transmission bandwidth for enhanced detectability and interference rejection in various digital communication, navigation, and radar systems [1]. In this paper, we consider the advantages and limitations of the application of acoustic surface-wave technology to spread spectrum systems. As a continuing theme to this discussion, we shall consider techniques for transmitting a digital data signal occupying a bandwidth considerably larger than required for the specified data rate. Three principal reasons for artificially enlarging the bandwidth of an information signal will be discussed in Section II. First, spread spectrum techniques permit a communication link to exhibit an attenuation against average power limited interfering signals that are not correlated with the particular waveform used to spread the spectrum. Such interfering signals might be deliberate jamming, random natural events, or even other users of the same spectrum. Second, signal-to-noise improvement even against receiver noise may be obtained by certain systems which make use of several codes; i.e., a given message may be communicated with a given reliability with less energy

Manuscript received November 2, 1972; revised November 27, 1972.
The authors are with Texas Instruments Incorporated, Dallas, Tex. 75222.